Coverage-dependent shifts of adsorbate features on the Cu(110)/oxygen surface

Coverage-dependent shifts of adsorbate features on the Cu(110)/oxygen surface

A Pantförder†, F Stietz†, A Goldmann† and R Courths‡

† Fachbereich Physik, Universität Gh Kassel, Heinrich-Plett-Straße 40, D-34132 Kassel, Germany
‡ Fachbereich Physik, Universität Gh Duisburg, D-47048 Duisburg, Germany

Abstract. We have studied atomic chemisorption at room temperature of oxygen on Cu(110) using high-resolution electron energy loss spectroscopy (HREELS) and angle-resolved ultraviolet photoemission spectroscopy (ARUPS). Both the oxygen vibration energy (HREELS) and the oxygen-induced antibonding orbital at about 1.4 eV below E_F (ARUPS) show well resolved shifts with oxygen coverage up to the completion of the (2×1)O overlayer. These are interpreted in terms of interchain lateral interactions.

1. Introduction

During the past few years, studies of surface structure and chemisorption have demonstrated that, in contrast to widespread earlier opinion, adsorbate-induced rearrangement of the outermost layer(s) seems to be the rule rather than the exception. This is in particular true for the open (110) faces of metals like Ni, Cu and Ag. An excellent review of our present understanding of oxygen chemisorption on these surfaces is given in [1].

Atomic oxygen on Cu(110) induces the 'added row' (2×1)O structure [2], where mobile Cu atoms diffusing across terraces and equally mobile oxygen atoms form linear O–Cu–O–Cu chains along the [001] direction, compare figure 1. An almost identical reconstruction is observed for Ag(110)(2×1)O. This could be expected, since these substrates are both isostructural and isoelectronic. However, while at room temperature only the Cu(110)(2×1)O geometry is observed for coverages $\leqslant 0.5$ monolayer (ML), on Ag a sequence of ordered $(n \times 1)$ LEED patterns appears, with n varying from seven to two as the coverage approaches 0.5 ML. There seems to be an intriguing difference between Cu(110) and Ag(110) with respect to the oxygen-induced reconstruction, which is not yet explained.

In an attempt to model the observed different behaviour Schimizu and Tsukada [3] recently calculated energetically optimized geometries of the added row model of Ag(110)$(n \times 1)$O for $n = 2$ and $n = 3$, as well as for Cu(110)(2×1)O. Important geometrical differences were indeed obtained. In particular on Ag(110) oxygen is predicted to be chemisorbed more weakly in (3×1) than in (2×1) geometry, and this different bonding strength was seen to cause a different vibration energy $\hbar\omega_\perp$ of the oxygen atom perpendicular to the surface. This paper stimulated two groups to check experimentally for such a shift with n [4,5]. Indeed both experiments clearly revealed shifts of $\Delta\hbar\omega_\perp = +0.9$ meV [4] and +0.7 meV [5], respectively, when going from $n = 3$ to $n = 2$, and these shifts agree within the given errors. However, the predicted shift is +5 meV, much larger than observed.
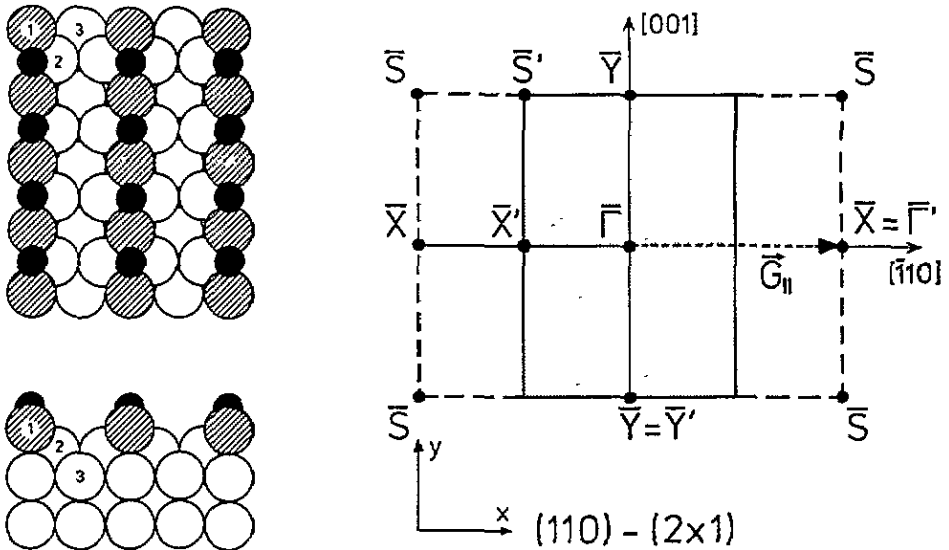
Figure 1. Left: top (upper) and side (lower) views of Cu(110)(2 × 1)O. Filled circles: oxygen; shaded: topmost copper row. Right: real-space directions *x*, *y* along the surface and corresponding 2D Brillouin zones of Cu(110), $\bar{\Gamma}\bar{Y}\bar{S}\bar{X}$, and of Cu(110)(2 × 1)O, $\bar{\Gamma}\bar{Y}\bar{S}'\bar{X}'$, respectively.

There may be several reasons for this discrepancy and a conclusive answer cannot be given at present. The calculations [3] indicate two relevant (and intrinsically connected) differences between the (3 × 1) and (2 × 1) geometries on Ag. One is the lateral displacement of the top substrate atoms just below the added row: in the (2 × 1) structure the two Ag atoms sitting below the oxygen atom along [1$\bar{1}$0] are displaced toward O by $\Delta = 0.1$ Å. The corresponding displacement for (3 × 1) is only 0.04 Å. According to [3] the increasing Δ at increasing coverage also increases the repulsive forces between added (*n* × 1) rows. In contrast, the calculation yields $\Delta = 0$ for Cu(110)(2 × 1)O, and the resulting absence of lateral forces indicates that there is no repulsion to keep the added O–Cu–O–Cu rows apart at low coverage. The other difference as calculated is the oxygen height above the Ag atoms in the added O–Ag rows: O atoms are bound higher (and more weakly) for (3 × 1) than for (2 × 1); in consequence $\omega_\perp$ changes. It might thus well be that the observed small $\Delta\hbar\omega_\perp$ is indeed related to a coverage-dependent change in surface geometry. However, as was pointed out in detail by Vattuone *et al* [4] a completely different interpretation works as well: assuming a simple electrostatic dipole–dipole coupling between the oxygen atoms also explains the data satisfactorily, without any assumptions on a distorted substrate/adsorbate geometry that changes with coverage.

To obtain further insight we decided to perform a combined HREELS and ARUPS study of coverage-dependent oxygen features on Cu(110) up to 0.5 ML. On this surface, the growth mechanism is different as compared to Ag(110)(*n* × 1)O: with increasing oxygen coverage, islands grow by aggregation of Cu–O–Cu–O strings and give rise to a local (2 × 1) reconstruction. At full coverage (0.5 ML) the islands have grown together and the whole surface is (2 × 1) reconstructed. Our results as described below indicate a close similarity to Ag and do not give any hint to a different interchain lateral interaction.

2. Experimental details

The HREELS spectrometer [6] was built for us by the group of H Ibach in Jülich. The UHV system where it is incorporated operates at a base pressure of $5 \times^{-11}$ mbar and is equipped with facilities for low-energy electron diffraction (LEED), x-ray-induced photoelectron spectroscopy (XPS) and standard sample preparation procedures. The Cu(110) sample was sputter cleaned by 700 eV Ar^+ ions and subsequently annealed at a temperature of $T = 620$ K. This procedure resulted in an excellent LEED pattern and no contaminations could ever be detected by XPS and HREELS. The HREELS spectrometer was operated with an incident beam energy $E_0 = 4.4$ eV, in specular reflection at $\theta = 60°$ with respect to the surface normal. The experimental full width at half maximum of the elastic peak was 3.9 meV. Signal averaging was employed and typical count rates are 4×10^4 s^{-1} in the elastic peak maximum. Adsorption was performed by admission of molecular oxygen at room temperature. A weak and diffuse $(2 \times 1)O$ pattern could be seen by LEED already at exposures around 1 L, while 10 L produced a very brilliant (2×1) image. No further increase of oxygen coverage or changes in the LEED and HREELS data could be detected for exposures up to 10^2 L.

The ARUPS results were obtained with an ESCALAB Mark II electrostatic energy analyser system built by Vacuum Generators. HeI radiation $(\hbar\omega = 21.2$ eV) was used to excite photoemission. Energy and angle resolution were set to $\Delta E = 80$ meV and $\Delta\theta = \pm 1.5°$, respectively. While the angle between photoelectron and incident photon was fixed to 38°, the sample normal was rotated in a plane perpendicular to the surface and containing both the electron and photon directions. Light polarization was achieved with a triple-reflection Au mirror polarizer and about 90% linear polarization (s or p polarized with respect to the plane containing the surface normal) could be obtained. The sample preparation was performed by Ar^+ ion bombardment at 500 eV and annealing at $T = 800$ K. The LEED results obtained after exposure to O_2 are in full agreement with those described above for the HREELS experiment.

3. Results and discussion

Since all HREELS spectra are taken in specular geometry, only vibrations perpendicular to the surface can be excited (dipole scattering [7]) and these correspond to the $\bar{\Gamma}$ point of the 2D Brillouin zone as defined in figure 1. Both energy loss and gain peaks were recorded. Their intensity ratio is determined by the Bose–Einstein distribution factor and the crystal temperature (always 300 K). The recording of both loss and gain features improves the accuracy with which the vibration energies may be derived from the spectra. On Cu(110)$(2 \times 1)O$ we observe the oxygen–metal stretch vibration at ± 49 meV, a surface phonon at ± 24 meV and (only indicated as a shoulder) another phonon around 13 meV. These results are in excellent agreement with earlier observations [8, 9] of this system and therefore we do not reproduce the spectra. They clearly parallel our data reported recently [5] from the essentially isostructural Ag(110)$(2 \times 1)O$ surface. In the following we will concentrate on the oxygen vibration.

Figure 2 shows the dependence on oxygen coverage of both the intensity and vibrational energy of the oxygen–metal stretch vibration. Not surprisingly the intensity varies linearly with coverage. However, also the oxygen peak energy shifts almost linearly. This loss peak is observable already at the very lowest coverage of about 1.5×10^{-2} ML (obtained around an exposure of 10^{-1} L), when the LEED pattern still shows the (1×1) periodicity
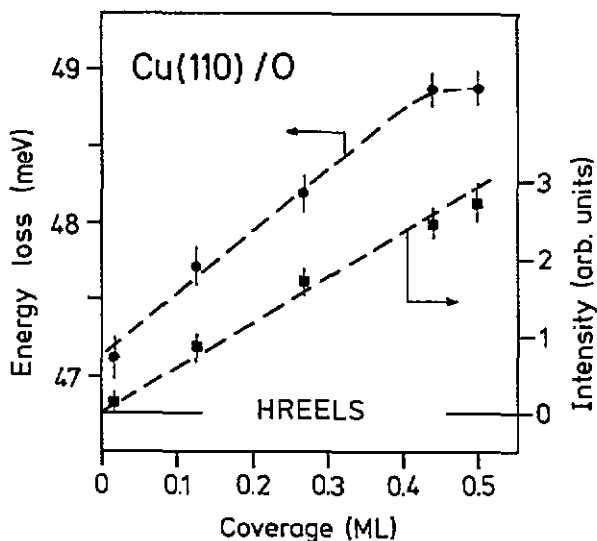
Figure 2. Loss energy (circles, left scale) and intensity (squares, right scale) of the oxygen–metal vibration observed after dissociative chemisorption on Cu(110).

of the unreconstructed substrate, and it exhibits a total energetic shift of (1.6 ± 0.2) meV until the completion of the (2×1)O reconstruction. However its experimental width of 6.2 meV does not change with coverage within the error margins. From this observation we conjecture that the width is not primarily determined by a different degree of surface disorder, but rather due to a coverage-independent vibrational damping.

Photoelectron spectra taken at the $\bar{Y}$ point of the surface Brillouin zone (compare figure 1) are reproduced in figure 3. The ordered overlayer system Cu(110)(2×1)O has already been studied in earlier work [10–12] and we refer here only to some relevant details. The (2×1)O surface is characterized by three bonding bands between 5 and 8 eV below E_F (labelled b_x, b_y and b_z in figure 3). Along the Cu–O–Cu–O chains their dispersion with $\bar{k}_\parallel$ is large [10–12], while it is almost zero perpendicular to that direction [10]. This behaviour reflects the strongly directional bond along the Cu–O rows. These bonding bands are accompanied by occupied 2D antibonding bands between the Cu 3d states (2–5 eV below E_F) and the Fermi edge. Two of them, labelled a_x and a_z in figure 3, have been identified unambiguously so far. In the present work, we have studied their behaviour with increasing oxygen coverage in some detail.

The clean Cu(110) surface supports an occupied surface state (label S in figure 3) at 0.4 eV below E_F, which shows p_y symmetry [13–15]. This peak disappears after completion of the 0.5 ML oxygen overlayer. Instead the adsorbate-induced peaks a_x (of odd symmetry along the $\bar{\Gamma}\bar{Y}$ azimuth) and a_z (even) are now observed. Their detailed shape and position at the $\bar{Y}$ point of the surface Brillouin zone are displayed in figure 4 as a function of coverage. Obviously the odd peak (a_x) shows a shift to higher initial state energies (lower binding energy) with oxygen coverage, while the even peak (a_z) does not move. Details, including the experimentally observed FWHM, are summarized in figure 5.

Within the completed (2×1)O surface, both occupied antibonding peaks show strong dispersion with $k_\parallel$ along $\bar{\Gamma}\bar{Y}$ [11, 12]. Both, with initial state energies $E_i = -1.2$ eV and -1.4 eV at $\bar{Y}$, disperse essentially in parallel by about 0.6 eV off E_F when going to $\bar{\Gamma}$. This is a clear indication that they are involved in the bonding along the Cu–O chains [10–12].
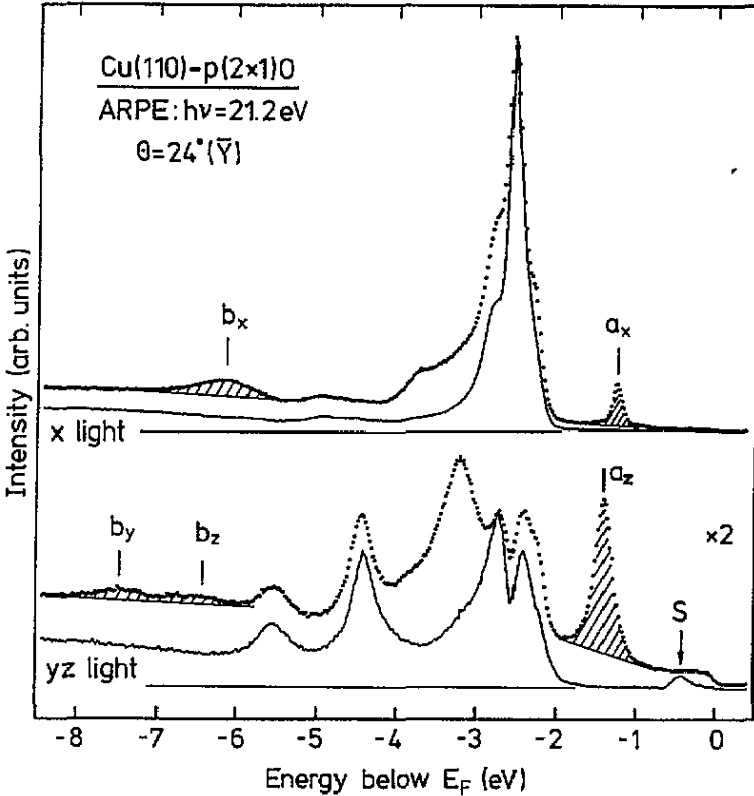
Figure 3. Angle-resolved photoelectron spectra taken along the $\bar{\Gamma}\bar{Y}$ azimuth at $\theta = 24°$, which corresponds to the immediate vicinity of the $\bar{Y}$ point (see figure 1 for definitions). Solid lines: clean Cu(110), dotted curves: Cu(110)(2 × 1)O. Linearly polarized radiation of $\hbar\omega = 21.2$ eV was used, with the E vector aligned along x (top panel, s polarization) and along yz (bottom panel, p polarization).

However, the initial state energy at $\bar{Y}$ of the even band is not at all affected by coverage, while the odd band shifts by about 0.2 eV which is about one-third of its dispersion along the chains.

Our interpretation of the results presented above is as follows. In accord with all structural studies [1] we assume that at 300 K a finite concentration of Cu adatoms exists on the terraces. An incoming oxygen molecule dissociates and one of its atoms traps a copper adatom thereby forming some kind of surface molecule located at an 'added row' site. Within this molecule odd (oriented along x) and even (y, z) states are energetically degenerate, in accord with the data in the lower panel of figure 5. This Cu–O surface molecule now traps a second Cu atom, since each O atom binds two of the low-coordinated Cu atoms [1] and further diffusing Cu and O atoms become trapped at the ends of already existing Cu–O–Cu rows. Thus a strong attractive Cu–O interaction along the [001] direction (y direction) is effective. With increasing length of such strings, a 1D dispersion along y is switched on, and the degeneracy between the odd and even states is lifted; this is observed in figure 5, lower panel, for coverages below 0.05 ML. With increasing coverage the 1D chains grow longer, up to 200 Å [1] and they are very mobile: they may diffuse as intact chains, although STM images indicate that they sometimes have a somewhat
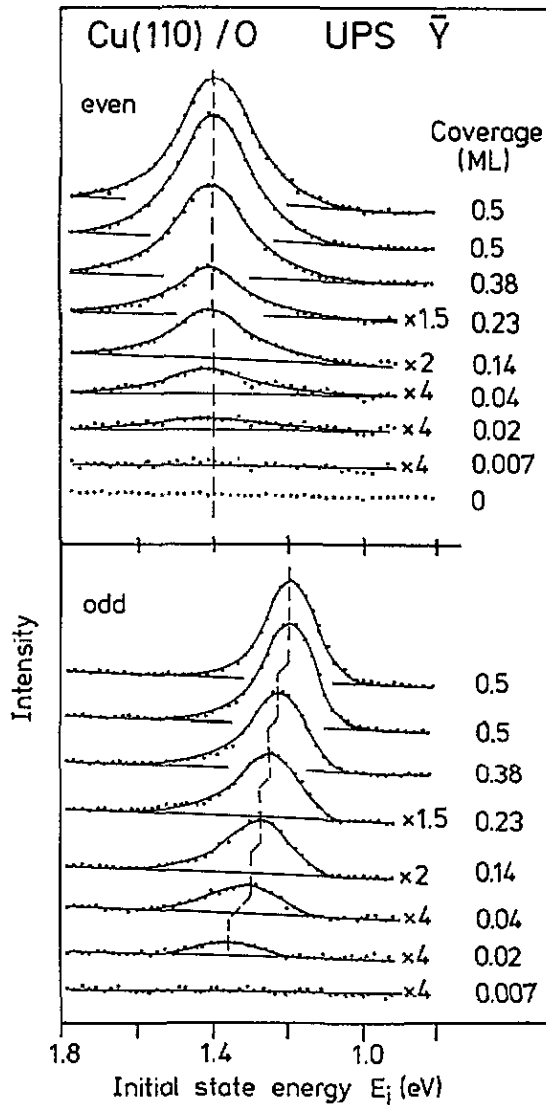
Figure 4. Angle-resolved photoelectron spectra taken at the $\bar{Y}$ point with linearly polarized radiation ($\hbar\omega = 21.2$ eV) at different oxygen coverages after room-temperature exposure. Top panel: even (a_z) state, bottom panel: odd (a_x) state.

irregular zig-zag appearance. Thus photoemission, which takes snapshots of the electronic structure in a time window small as compared to diffusion steps, probes somewhat distorted geometries. When the chain density increases further the added rows agglomerate into (2×1) reconstructed anisotropic islands, with a long/short coherence length along the y/x directions, respectively. Thus, an attractive interaction (weak as compared to the bonds along y) exists between the chains along x. As is evident, the agglomeration of a second chain to an already present chain most sensitively influences the odd adsorbate states oriented perpendicular to the chains. In fact, at coverages between about 0.1 and 0.3 ML there are long islands of different widths along y simultaneously present on the surface,
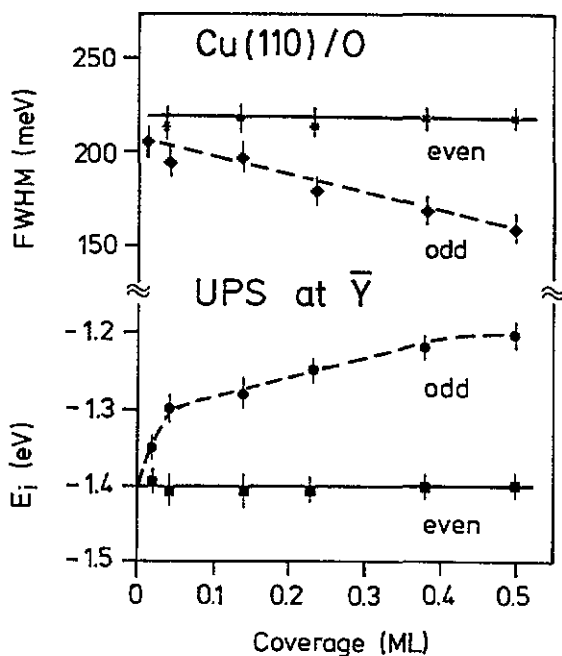
Figure 5. Peak positions (bottom curves) and experimental full widths at half maximum (top curves) of the odd (a_x) and even (a_z) antibonding peaks observed in figure 4.

causing different dispersion of the odd bands. In consequence, different dispersion curves superimpose, and this is reflected in the rather large width of the odd photoemission peak (upper half of figue 5). After the whole surface is covered by $(2 \times 1)O$, there is only one odd state distributed homogeneously over the sample. Therefore the experimental FWHM attains a minimum now. The width of the even state is not changed at all, since it reflects essentially the dominant interaction along the chains, which is not seriously affected by agglomeration into a (2×1) arrangement.

The interchain interaction shifts the odd (x-like) band observed in UPS nearer to E_F. This band is formed by hybridized Cu 3d and O 2p orbitals and is of 'antibonding' character [10–12]. Its shift to E_F therefore indicates a strengthening of the chemisorptive bond. This is exactly what is seen also in the HREELS data. The latter spectroscopy monitors vibrations perpendicular to the substrate surface and should be particularly sensitive to the z-like orbitals. Strengthening the bonds with increasing coverage shifts the loss peak to larger energies, and this is clearly observed in figure 2. Since figure 5 demonstrates that the even band observed in ARUPS does not react to increasing coverage, we identify this band with the dominant (y-like) Cu–O bond directed along the chains. Thus the combination of HREELS and UPS helps us to a consistent interpretation of the various directed orbitals and their changes with oxygen coverage.

We add two further pieces of information. First, it is well known from STM studies [1] that the $(2 \times 1)O$ surface of Cu(110) prepared by chemisorption at 300 K contains steps, domain boundaries and other types of defect. We have therefore also annealed our samples to about 370 K, which creates a much more perfect (2×1) structure with large flat terraces [1]. We noted that our results are not changed by that treatment. Obviously these defects play a minor role in our experiments, which average out many of their contributions.

Second, we have also observed a shift (≈ 0.1 eV) to E_F of the corresponding antibonding peak in ARUPS from Ag(110) when the coverage increases up to 0.5 ML. However, on Ag(110)($n \times 1$)O the x- and y-like peaks cannot clearly be separated experimentally and therefore the results are not as transparent as in the present case of Cu(110)/O.

In conclusion both Ag(110) and Cu(110) behave in complete analogy with respect to the coverage-dependent shift of the oxygen–metal vibration energies and the occupied antibonding adsorbate orbitals. Also the surface phonons show very similar shifts to higher vibration frequencies with coverage on both Ag [5] and Cu. Our results on phonons are in full agreement with those reported in [8, 9] and are therefore not reproduced here. We note, however, that the coverage-dependent shifts presented in this paper have not been observed before. From our results no evidence is obtained that on Cu(110) and Ag(110) different electronic stabilization mechanisms between the metal–oxygen chains might be operative. This supports considerations by Vattuone *et al* [4] that the predicted structural differences for both adsorption systems [3] are not proven yet by experimental evidence. We must state that the question as to different growth mechanisms of (2×1)O on Cu and Ag remains an open and still intriguing problem.

Acknowledgments

References

[1]   Besenbacher F and Norskov N K 1993 *Prog. Surf. Sci.* **44** 5
[2]   Coulman D J, Wintterlin J, Behm R J and Ertl G 1990 *Phys. Rev. Lett.* **64** 1761
[3]   Schimizu T and Tsukada M 1993 *Surf. Sci.* **295** L1017
[4]   Vattuone L, Valbusa U and Rocco M 1994 *Surf. Sci.* **317** L1120
[5]   Stietz F, Pantförder A, Schaefer J A, Meister G and Goldmann A 1994 *Surf. Sci.* **318** L1201
[6]   Ibach H 1991 *Electron Energy Loss Spectrometers (Springer Series in Optical Sciences 63)* (Berlin: Springer) p 5
[7]   Ibach H and Mills D L 1982 *Electron Energy Loss Spectroscopy and Surface Vibrations* (New York: Academic)
[8]   Baddorf A P, Mundenar J M and Plummer E W 1986 *J. Electron. Spectrosc. Relat. Phenom.* **38** 219
[9]   Mundenar J M, Baddorf A P, Plummer E W, Sneddon L G, Didio R A and Zehner D M 1987 *Surf. Sci.* **188** 15
[10] Didio R A, Zehner D M and Plummer E W 1984 *J. Vac. Sci. Technol.* A **2** 852
[11] Courths R, Cord B, Wern H, Saalfeld H and Hüfner S 1987 *Solid State Commun.* **63** 619
[12] Hüfner S 1995 *Photoelectron Spectroscopy—Principles and Applications (Springer Series in Solid-State Sciences 82)* (Berlin: Springer) p 336
[13] Kevan S D 1983 *Phys. Rev.* B **28** 4882
[14] Chen C T and Smith N V 1989 *Phys. Rev.* B **40** 7487
[15] Smith N V and Chen C T 1991 *Surf. Sci.* **247** 133